# SFM Characterization of Poly(isocyanodipeptide) Single Polymer Chains in Controlled Environments: Effect of Tip Adhesion and Chain Swelling

**Wei Zhuang,[†] Christof Ecker,[†] Gerald A. Metselaar,[‡] Alan E. Rowan,[‡] Roeland J. M. Nolte,[‡] Paolo Samorí,*[,†,§,∥] and Jürgen P. Rabe*[,†]**

*Department of Physics, Humboldt University Berlin, Newtonstrasse15, 12489 Berlin, Germany, Department of Organic Chemistry, NSR center, University of Nijmegen, Toernooiveld, 6525 ED Nijmegen, The Netherlands, Instituto per la Sintesi Organica e la Fotoreattività, C.N.R. Bologna, via Gobetti 101, 40129 Bologna, Italy, and Nanochemistry Laboratory, Institut de Science et d'Ingènierie Supramolèculaires (ISIS), Université Louis Pasteur of Strasbourg, 8 allée Gaspard Monge, 67083 Strasbourg, France*

*Received June 19, 2004; Revised Manuscript Received November 5, 2004*

ABSTRACT: Isolated slightly hydrophilic chains of poly(isocyanodipeptides) (PICs) adsorbed on mica were studied by intermittent contact mode−scanning force microscopy (IC−SFM) in an ambient atmosphere controlled both with respect to the relative humidity (RH) and the presence of $CHCl_3$ vapor. SFM revealed that the average chain height increases up to more than an order of magnitude with decreasing RH, leading to the highest value at RH = 0%. This is due to both a minimization of the capillary forces between the SFM tip and the hydrophilic substrate surface and a collapse of the side chains in the poor solvent. In a saturated $CHCl_3$ vapor atmosphere, the chain heights increase up to twice this value, which is close to the polymer diameter measured by powder X-ray diffraction. This indicates that the PIC chains are solvated by $CHCl_3$ molecules, causing the swelling of the single polymers. Achieving a control over the thickness of the polymer chains is fundamental for their optimal observation by SFM. Moreover, the understanding of the conformational properties of single macromolecules adsorbed on surfaces under different environmental conditions is of importance for unraveling their physicochemical properties and their dynamics, including their reactivity.

## Introduction

Intermittent contact mode−scanning force microscopy (IC−SFM), known also as tapping mode SFM,[1] offers direct access to the structural and mechanical properties of single macromolecules[2−4] as well as to supramolecular architectures[5] adsorbed on a surface. It is a valuable method for the investigation of soft organic and biological layers, since it applies very small lateral forces to the sample surface.[1] However, the measurements of the heights of the adsorbed molecules, which are typically performed at the solid−air interface, are not easily reproducible and the obtained values are far smaller than the diameters of the investigated molecules themselves.[3,6,7] This can even lead to such small chain's heights that these are hardly detectable by SFM. To overcome this problem contrasting agents have been added to the polymers,[8] altering in this way their physicochemical properties. Besides, Van Noort et al. introduced a model describing the relationship between the height anomalies in IC−SFM at the solid−air interface and the tip−sample adhesion caused by capillary force.[9] This experimental finding prompted us to find new routes to avoid height anomalies in IC−SFM imaging of neat macromolecules adsorbed at surfaces by removing the capillary force.

The capillary forces caused by tip−sample adhesion have been systematically studied in contact mode SFM.[7,10] The curvature at the contact between the SFM tip and the sample causes the formation of a "water neck", namely the condensation of vapor from the ambient atmosphere. Also surfaces exposed to air are typically coated by a layer of water, whose thickness depends on the relative humidity (RH) of the atmosphere and on the physicochemical nature of the components.[11] It can result in a strong attractive capillary force ($10^{-7}$−$10^{-8}$ N) that holds the tip in contact with the surface.[10] To avoid capillary forces the ambient relative humidity should be zero, although some previous work on the tip−mica system has demonstrated that below RH = 10% the capillary forces do not further decay.[12] Thus, two experimental procedures to minimize the effect of capillary forces can be followed: the first is to flood a sealed measurement chamber with a dry inert gas such as $N_2$, He or Ar; the second is to perform measurements with both the tip and the sample immersed in a liquid medium making use of a fluid cell.[10] Both have been undertaken for visualizing hydrophilic macromolecules, such as double stranded (ds) DNA.[13] It was found that the apparent height of ds-DNA decreases with increasing ambient humidity, which was ascribed to the capillarity forces.[7,14] Differently, at the solid−liquid interface the height of DNA was 0.6 nm higher than that of ds-DNA measured in ambient air.[15] If one wishes to apply the liquid medium approach to macromolecules soluble in organic solvents, an aqueous solution becomes impractical for molecular conformation studies and an organic solvent is required for the SFM experiment.

A series of peptide based poly(isocyanides) has recently been synthesized and their unique physicochemical properties (including the mechanical ones), have been reported. [3,16]

[†] Humboldt University Berlin.
[‡] University of Nijmegen.
[§] C.N.R. Bologna.
[∥] Université Louis Pasteur of Strasbourg.
* Corresponding authors: (J.P.R) fax, +49-(0)30−20937632; e-mail, rabe@physik.hu-berlin.de; (P.S.) fax, +39-051-6399844; e-mail, samori@isof.cnr.it.

10.1021/ma048786z CCC: $30.25 
Published on Web 12/30/2004

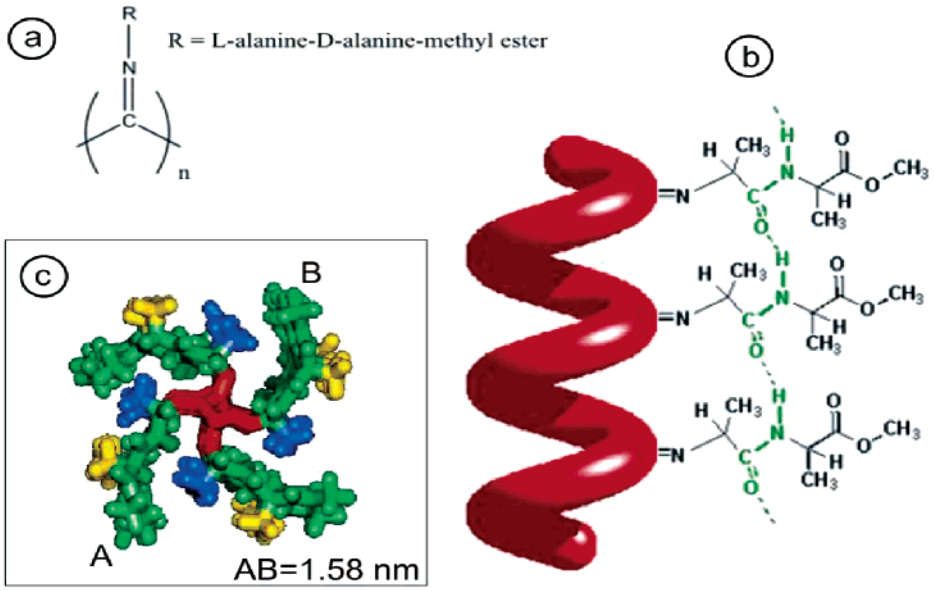


**Figure 1.** (a) Chemical formula of the poly(isocyanide) bearing L-alanyl-D-alanine methyl ester side groups. (b) Hydrogen-bonded array formed between the sidearms. (c) Molecular model of the L,D-PIAA $4_1$ helix; the rod diameter 1.58 nm results from the end-to-end distance of two opposite end groups in the sidearms (A−B).

**Scheme 1. Side View of the Liquid Cell Using the "Water Cover" Method**

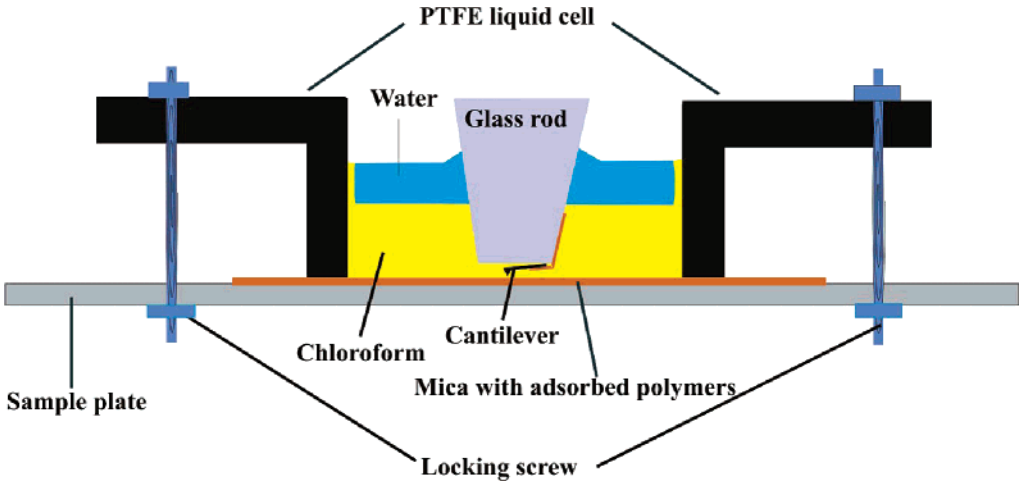


A poly(isocyanide) derivative bearing L-alanine-D-alanine methyl ester side groups (L,D-PIAA) (see Figure 1a) was found to be ideal for the studies proposed above, due to its solubility in organic solvents and its slightly hydrophilic character.[17] This polymer was recently investigated by IC−SFM under ambient conditions.[3] PIAAs were synthesized either with a $Ni(ClO_4)_2 \cdot 6H_2O$ salt (Ni−PIAA) or trifluoroacetic acid ($H^+$−PIAA) as a catalyst.[16,18] Although the $H^+$−PIAAs exhibited much longer contour lengths than the Ni−PIAAs, both types of polymers equilibrated in 2D possessed the same persistence length, viz. 76 ± 6 nm.[3] This high rigidity is due to the $4_1$ helical backbone of the polymer and the hydrogen bonding network formed between the pendant alanine-groups (see Figure 1b). The average chain's thickness obtained from the SFM exploration at the solid−air interface amounted to 0.30 ± 0.06 nm.[3] This value is much lower than the 1.58 nm diameter of the PIAA rod (that corresponds to the diagonal A−B of the square-shaped cross-section in Figure 1c) as determined by both powder X-ray diffraction,[16] and also lower than the edge length which amounts to $\sqrt{2}/2 \times 1.58$ nm = 1.12 nm, being the side of the square in the projection of the polymer structure. Hence, the investigation of the conformation of PIAA on the solid surface, and in general of hydrophobic or slightly hydrophilic chains on a hydrophilic surface, as a function of different measurement conditions is of great interest.

Here we describe an IC−SFM exploratory study, performed under different and controlled environmental conditions, on the conformation of Ni-L,D-PIAA chains adsorbed on a mica surface. The controlled environmental conditions included extremely low and high humidity, organic solvent vapor and liquid solvent.

## Experimental Procedures

Chloroform ($CHCl_3$) is a very good solvent to dissolve Ni−PIAA; moreover, due to its relatively high volatility at room temperature, it can be easily used to saturate an environment with its vapors. A solution (50 $\mu$L) of 1 mg/L Ni−PIAA in $CHCl_3$ was spin-coated onto a freshly cleaved muscovite mica surface, employing a spinning rate of 50 rps for 30 s.

Topographical SFM images were recorded with a Molecular Imaging PicoSPM scanning force microscope (MI−SFM)[19] operating in intermittent contact mode. Nanosensors Point-probe silicon cantilevers were used with a spring constant of 2.8 N/m. While the typical resonance frequency both in air and in vapor environment was 71−85 kHz, in liquid $CHCl_3$ it

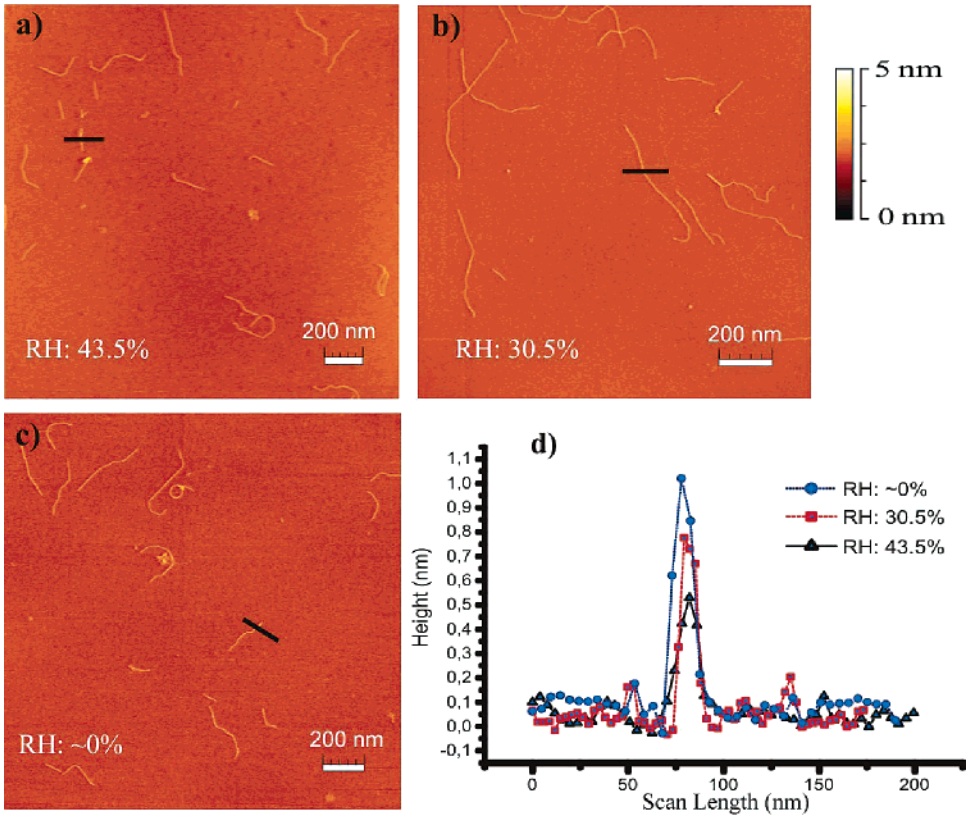


**Figure 2.** IC−SFM height images and their cross section analysis of isolated chains Ni−PIAA chains visualized at the solid−air interface at (a) RH = 43.5%, (b) RH = 30.5%, and (c) RH = ~0% (d) Cross-sections traced along the black lines on image (a, triangle symbol), (b, square symbol) and (c, dot symbol).

amounted to 20−30 kHz. Results were reproduced using RTESP Si probes (Digital Instruments).

A hermetically sealed environmental chamber installed on the MI−SFM was employed to control the environment during the measurements. A Testo hygrometer probe was inserted into the chamber to monitor the RH in-situ with an accuracy better than ±2%. To obtain extremely low ambient humidity, the chamber was filled with dry helium gas. The gas was kept flowing through the chamber for 1 h until the RH reached 0−2%, and then a gentle flow was also maintained during the course of the measurements. To attain a controlled high relative humidity in the environmental chamber, an aqueous $CaCl_2$ solution was inserted in the chamber:[4e,20] a low concentration of such $CaCl_2$ solution generates a high relative humidity. The sample was placed above the solution and maintained in such a fixed RH environment for 2 h to ensure equilibration.

The same setup was also used for the measurements under $CHCl_3$ vapors. Two Petri-dishes filled with $CHCl_3$ were placed in the chamber under the sample: in about 30 min time the chamber was saturated with $CHCl_3$ vapor. The hygrometer sensor and any other corrodible material were removed or protected from getting in contact with the $CHCl_3$ vapor.

For imaging in a liquid environment, a liquid cell made of Teflon was employed to resist the corrosion from $CHCl_3$ (Scheme 1). Water, having a lower vapor pressure, was covering the $CHCl_3$ to prevent its evaporation. Nevertheless, due to the favorable interfacial interactions between $CHCl_3$ and Teflon, if compared to those between water and Teflon, a minor part of the $CHCl_3$ adjacent to the Teflon wall was not covered by water; hence, $CHCl_3$ could evaporate, albeit very slowly. This setup allowed SFM studies to be performed at room temperature in a stable condition for at least 1 h.

The molecular height can be evaluated from the topographical profiles in the SFM images. To obtain precise and reliable average data, a new procedure[21] was developed, which allows one to determine the cross sections between every 1−2 pixels on the images recorded with a 512 × 512 pixels resolution. In this way, on a chain with a contour length of 200 nm visualized in a SFM image acquired with a size of 1500 × 1500 $nm^2$, about 60 cross sections are sampled along the chain's contour.

A large set of data were collected from different measurements, and three different types of averages were determined: (i) "total average height", which considers all the data from all the measurements in one specific controlled environmental condition; (ii) "measurement average height", which takes into account the data from all the images in one measurement, e.g. the images recorded in different locations of the same sample with the same tip, similar tapping force and identical environmental condition; (iii) "maximum average height", which includes the data from one image, being the highest contrast image obtained in a given controlled environment. We will present and discuss only the "measurement average height" and "maximum average height" since the "total average height" exhibited a relatively large standard deviation (error bar). We have recorded 10−12 images per measurement, and in each image there were about 10−15 polymer chains to be analyzed. We have collected a large number of cross sections on each chain. The precise number of them depends on the chain length and on the image scale length, given that the cross sections were measured every 1−2 pixels.

## Results

**Height Evaluation at Different Relative Humidity.** Figure 2 shows the topographical SFM images of isolated Ni−PIAA chains measured in air at different relative humidities and the relative cross sections traced on single chains. The "maximum average height" value determined from about 600 data points on every image, resulted in the following: 0.56 ± 0.06 nm for RH = 43.5%, 0.71 ± 0.09 nm for RH = 30.5%, and 0.84 ± 0.11 nm for RH = 0%. A similar trend was observed following the behavior of a given chain changing in situ the environmental condition (see Supporting Information).

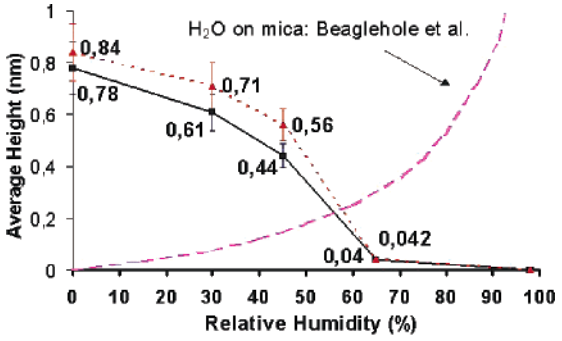


**Figure 3.** "Maximum average height" (dotted line, triangle symbol) and "measurement average height" (solid line, square symbol) of PIAA measured by IC−SFM vs the relative humidity. The error bar was determined using different chains in the same image. The dashed line shows the ellipsometrically determined thickness of water on mica as a function of humidity, according to Beaglehole and Christenson.[11]

We performed our studies also under high humidity environments; this was done by adding a defined aqueous solution of $CaCl_2$ into the environmental chamber. We obtained a "measurement average height" of 0.44 ± 0.05 nm at RH = 43% and 0.040 ± 0.009 nm at RH = 64%. Thus, the measured height decreased by about 0.40 nm, i.e., 1 order of magnitude, with increasing relative humidity. At RH = 98%, we were not able to observe the molecules any more.

**Height in Chloroform Environment.** The maximum average height of 0.84 ± 0.11 nm measured under extremely low humidity conditions is still much smaller than the polymer rod diameter determined by powder X-ray diffraction, which amounts to about 1.58 nm. We decided therefore to extend our studies to PIAA under a good solvent condition, namely $CHCl_3$, by investigating the ultrathin film at the solid−$CHCl_3$ vapor interface.

Figure 4 displays SFM images and relative topographical profiles of PIAA in air and in a saturated $CHCl_3$ vapor. The data reveals an increase of the height of the polymer chains by ca. a factor of 2 going from ambient air to $CHCl_3$ vapor. Under the latter condition the "measurement average height" and "maximum average height" amounted to 1.09 ± 0.18 and 1.47 ± 0.32 nm, respectively. The IC−SFM investigation of the PIAA chains at the solid−liquid interface in a $CHCl_3$ solvent using the previously described "water cover" method did not allow to visualize the strands adsorbed at the surface, but it revealed only some moving traces. Similarly, for a positively charged dendronized polymer on mica,[22] only a few chains adsorbed on the substrate could be observed by SFM at the interface between the solid surface and a solution in $CHCl_3$. It indicates that the competition between adsorption on mica and solvation in $CHCl_3$ favored the latter. In this scenario, a few positively charged dendronized polymers adsorb on the polyelectrolyte mica surface due to relatively strong ionic interactions. On the other hand, since the PIAA molecules are more neutral, it can be expected that they prefer to be dissolved in the supernatant solution in $CHCl_3$.

## Discussion

The height of the Ni−PIAA molecules under different environments has been systematically investigated by IC−SFM. Figure 5 shows the maximum average height and the measurement average height collected under different environmental conditions.

**Height Anomalies Caused by Adhesion.** Previous studies on the negatively charged ds-DNA assembled on a hydrophilic ionic mica surface revealed the presence of capillary forces between the water layer adsorbed on the surface and the SFM tip. This led to the formation of a meniscus between the tip and the sample surface, which played a paramount role in the thickness determination of the ds-DNA molecule under different humidities.[7,23] Instead of the hydrophilic ds-DNA, we employed IC−SFM on the hydrophobic PIAA molecule; hence, here the capillary force on the sample should not depend on the humidity.

The recently developed Van Noort model[9] seems to be more suitable to explain our experiments. According to this model, since the water wets preferentially the mica rather than the slightly hydrophilic PIAA molecule, the tip oscillation amplitude on the PIAA is not influenced by the thin water layer.[24] Therefore, the artifacts in the height caused by the adhesion between the tip and the PIAA can be excluded. On the other hand, it was shown that height measurements performed with IC−SFM could have errors up to 10 nm if the difference in adhesion force is sufficiently large.[9] This is due to the distorted oscillation of the SFM cantilever caused by the adhesion between the tip and the mica surface during its swing. In this way, surfaces with a large adhesion force are expected to appear higher in topography. As known, under ambient conditions the main contribution to the adhesion forces is the capillary force caused by a water layer, which strongly depends on its thickness.[7]

On the other hand, Beaglehole et al. reported on the relationship between the RH and the thickness of the adsorbed water layer on mica.[11] Ellipsometric data (see Figure 3) revealed that the water layer thickness grows more or less linearly below ∼45% RH, whereas an exponential increase occurs at RH higher than 45%. Thus, the model introduced by Van Noort can explain well the reversed proportional relationship between the measured molecule height and the thickness of water on mica, as shown in Figure 3. By and large, at extremely low humidity conditions the thickness of the water layer on mica is minimized; consequently the adhesion between the tip and surface is minimized. The proper visualization of the mica background was the basis for an artifact-free determination of the PIAA heights. With the increasing water layer thickness up to saturation, the apparent height of PIAA decreased dramatically until the resolution got lost.

**Indentation and Tip Broadening Effect.** SFM resolution in the imaging of molecular samples is also determined by several other factors, including the applied damping force, tip geometry, scan speed, and the frequency-dependent viscoelastic properties of the samples. In our experiment we always chose moderate scan rates (1.8−3 Hz), being in the range of scan speeds for high-resolution imaging.[25] Since our investigated molecular system (PIAA) is an extremely stiff molecule, the viscoelastic properties may be neglected.

However, the effects of the indentation due to the applied damping force and to the tip geometry are not negligible. The IC−SFM was operated with a set-point, which typically results in a more than 200 nN peak force (the maximum force occurring when tip is tapping the surface).[26] This is a rather large force that can produce

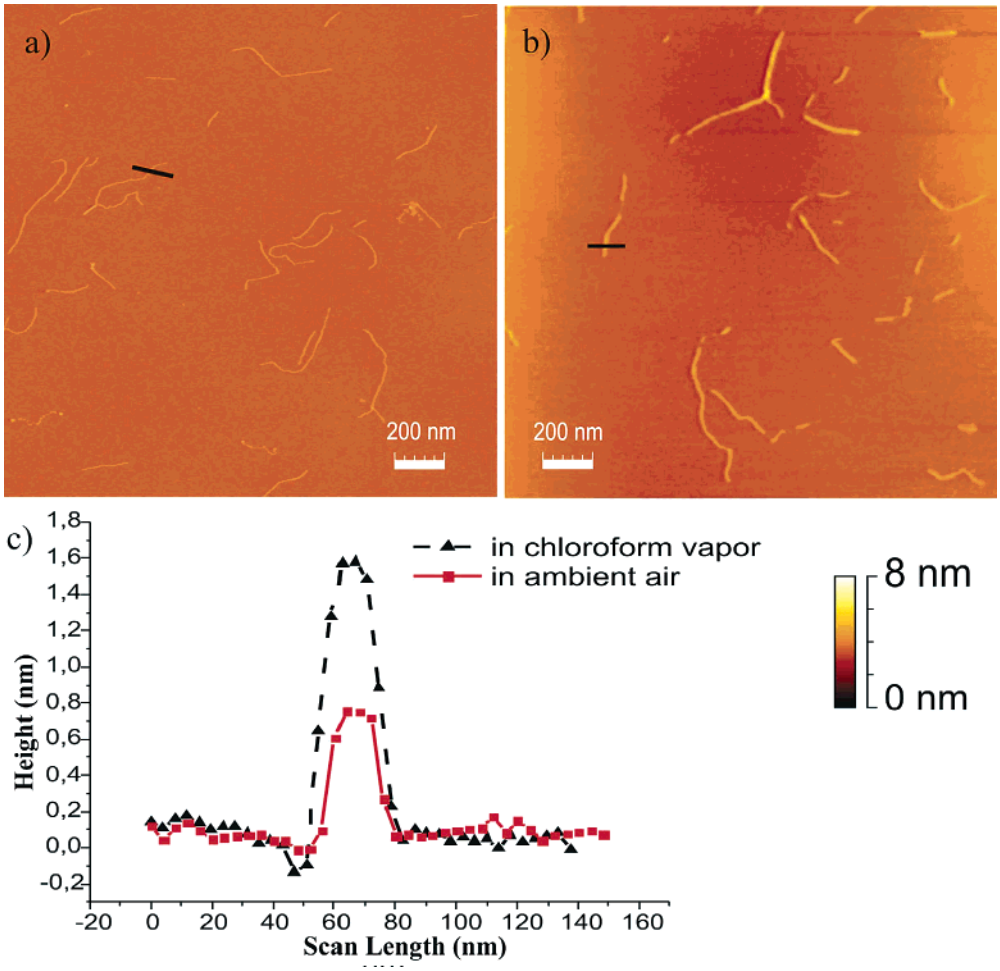


**Figure 4.** IC−SFM height image of PIAA sample recorded (a) in ambient air, and (b) in a $CHCl_3$ saturated chamber. (c) Cross-section analysis on the traced lines: from part a, marked with solid line, square symbol, and from part b, with dashed line, triangle symbol.

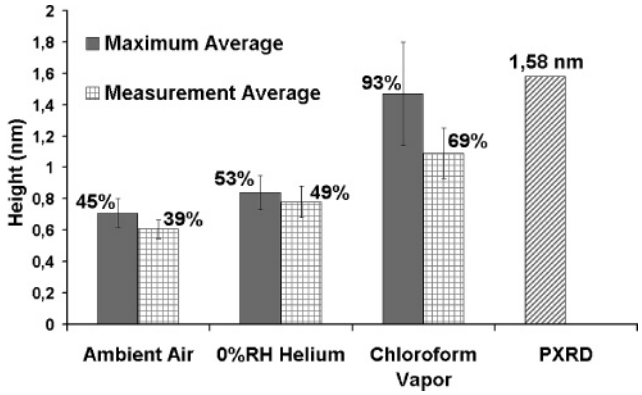


**Figure 5.** Heights of PIAAs under different conditions as measured by IC−SFM. The maximum average height (filled) and measurement average height (squared) are depicted together with their error bars. On the right the PIAA height measured by powder X-ray diffraction (oblique) is shown. On the top of each bar the ratio of the height measured by IC−SFM and by PXRD is given.

an indentation into the sample. We always tried to operate with the maximum set-point which allowed good images to be obtained. On the other hand, according to the Van Noort model, the increased damping results in a larger deviation from a sinusoidal swing, thus leading to a larger adhesion effect, negatively affecting the reliability in the topographical imaging.[9]

Furthermore, the "tip broadening effect" occurring while imaging could play a role in the height measurement. The tip prior to being used is known to possess a terminal radius smaller than 10 nm. Considering a broadening taking place during imaging to a 20 nm radius, the area under the tip becomes 4 times that of the initial one. Because of this area increase, the pressure (force per unit area of mica) is lower. Therefore, a sharp tip indents more into the mica surface than a broad tip.[27] Nevertheless, since the diameter of our molecule is only ca. 1 nm, the area on the molecule, which supports the tapping force and disperses the energy, is very small compared to the area on mica. This small area leads to a high pressure and hence it can be expected that the tip indentation on the PIAA molecule is always deep using either a sharp or a broad tip. In a different manner, on the mica surface the indentation will be higher when the tip is sharp (initial states of the imaging) and lower when the tip is broad. This difference caused by the tip broadening effect influences the height measurement and leads to lower molecular height values when a broad tip is used. The indentation and "tip broadening effect" cannot be avoided in most cases. Therefore, they contribute to the overall error bar in the average height determination.

**Role of the Solvent.** In the presence of $CHCl_3$ an average height of 93% of that obtained by X-ray diffraction was determined. This result is most likely due to the swelling of the chains occurring in the presence of

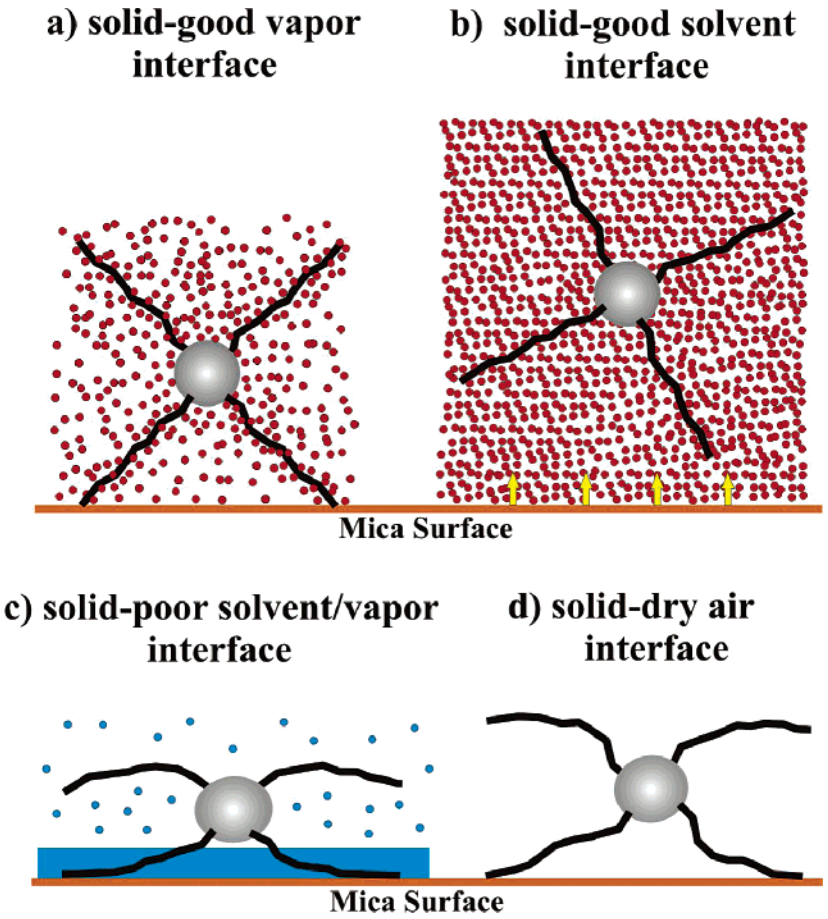


**Figure 6.** Schematic drawing of the cross-sectional views of PIAA rods (a) at the mica−good vapor interface, (b), at the mica−good solvent liquid interface, (c), at the mica−poor solvent interface under the condition of ambient air, (d) at the mica−dry air interface. Different possible conformations of the sidearms are shown. The red dots in parts a and b represent chloroform, and the blue dots and rectangle in part c represent water vapor and liquid layer, respectively.

a good solvent that gets incorporated among the sidearms. In an environment saturated with the $CHCl_3$ vapor, due to a strong affinity, the $CHCl_3$ molecules occupy the volume between the sidearms or even the surrounding space (see Figure 6a). This forces the sidearms to adopt a stretched conformation leading to a polymer height which is close to the polymer rod diameter, the latter resulting from the end-to-end distance between two symmetrically sidearms in the ideal energy minimized model structure. Furthermore, the investigation at the solid−liquid interface reveals that, due to a more favorable interaction between $CHCl_3$ and the polymer rather than between the substrate and the polymer, the latter is desorbed from the mica surface and fully solvated in $CHCl_3$. Since the molecule appears to adopt conformation with stretched sidearms in the presence of a saturated $CHCl_3$ atmosphere, it is most likely that at the solid−liquid interface the sidearms are also stretched as shown in Figure 6b.

The behavior of the PIAA chains measured in the presence of water liquid and vapor is different. Besides the key role played by the height anomalies of the PIAA chains adsorbed on mica caused by the adhesion of the tip on a water coated mica, a significant role is also played by the solvent−solute interaction. In the present case of a poor solvent it is very likely that the PIAA side chains adopt a collapsed conformation (Figure 6c), leading to small chain heights, as determined by SFM analysis.

In contrast, the measurements in solvent-free environment, i.e., at the solid-dry air interface, revealed larger heights than in ambient air. In this case the sidearms are still not extended but the effect of the capillary force on mica and the collapse of side chains in poor solvent are possibly minimized as shown in Figure 6d. The scenario is quite complicated since it involves a net force resulting from the mica adsorption force, the hydrogen bonds between neighboring side chains, and the repulsive force between side chain arrays. Thus, it is not possible to fully explain the role played by each of these effects.

An important contribution to the SFM measurements could possibly come from the different mechanical properties of the polymers under the various environments. This contribution should also be reflected in the SFM determination of the chain heights as a result of the force interactions between the two bodies. Further studies are required to confirm this.

It should be noted that the model presented here is not necessarily the only reason for the increase of the height under $CHCl_3$ vapor conditions. In fact other uncontrolled contributions from tip indentation or tip−mica adhesion effects might be changed in $CHCl_3$ vapor environment and thus should be taken into account. Moreover, it will be very interesting to extend these kinds of studies on different substrates. In our case, we have not been successful to perform the same experiments on a hydrophobic surface as highly oriented pyrolitic graphite (HOPG) due to the poor tendency of these PIC chains to adsorb on graphite. Nevertheless preliminary experiments on an alkylated dendronized polymer revealed that the swelling of the chains occurs

also on HOPG.[28] It is very likely that on such a hydrophobic substrate the effect of the humidity is less pronounced.

Although the swelling behavior in chloroform vapor at a first glance appears to be a simple process, it is most likely to be characterized by a very complicated mechanism. To cast light onto this issue, computer simulations on the adsorption of the PIAA on mica in the presence of chloroform will be undertaken in the near future.

## Concluding Remarks

IC−SFM offers direct access to the conformational properties of neat single polymer chains adsorbed at surfaces. The precise measurements of the polymer chain heights can be influenced by several factors, among them the adhesion between tip and substrate plays a crucial role.

By using of an environmental chamber, we were able to carry out an IC−SFM investigation on stiff, slightly hydrophilic PIAA chains on mica in controlled ambients. At different humidities, the SFM measurements gave different average heights of the macromolecules. In the medium and low humidity range, the measured apparent height of PIAAs showed a nearly reversed proportional linear relationship with the ambient humidity. In the high humidity range, the apparent height abruptly decreased until it completely vanished. This is well described by both the effect of tip−mica adhesion introduced in the Van Noort model and the collapsed conformation adopted by the sidearms in the presence of the poor solvent.

In the presence of a good solvent, IC−SFM revealed a swelling of the chain due to the inclusion of solvent molecules among the sidearms. This led to a chain height corresponding to 93% of the value obtained by X-ray crystallography, and the average result revealed a nearly 2-fold increase of the height measured in ambient air. This suggests that after minimizing the influence from the humidity and the SFM tip, the interaction of a single macromolecule with a solvent is reflected in the height measurement. The controlled introduction of organic solvent represents a new approach to study the conformation and dynamic swelling behavior of single macromolecules or macromolecular nanostructures by SFM. This opens new routes for the nanoconstruction at surfaces.

**Acknowledgment.** This work was supported by the EU-TMR project SISITOMAS (project reference FMRX970099), by the European Science Foundation through the SMARTON program as well as by the SONS−BIONICS project, and by the Deutsche Forschungsgemeinschaft (Sfb448 "Mesoskopisch strukturierte Verbundsysteme"). We thank M.B.J. Otten, I. Gössl, J. Barner, and N. Severin for useful discussions.

**Supporting Information Available:** Text and figure describing TM-SFM height images and how they were obtained. This material is available free of charge via the Internet at http://pubs.acs.org.

## References and Notes

(1) (a) Zhong, Q.; Inniss, D.; Elings, V. *Surf. Sci.* **1993**, *290*, 688−692. (b) Bustamante, C.; Keller, D. *Phys. Today* **1995**, *48*, 32−38. (c) Tamayo, J.; García, R. *Langmuir* **1996**, *12*, 4430−4435. (d) Takano, H.; Kenseth, J. R.; Wong, S. S.; O'Brien, J. C.; Porter, M. D. *Chem. Rev.* **1999**, *99*, 2845−2890.

(2) (a) Sheiko, S. S.; Möller, M. *Chem. Rev.* **2001**, *101*, 4099−4123. (b) Schlüter, A. D.; Rabe, J. P. *Angew. Chem., Int. Ed.* **2000**, *39*, 864−883.

(3) Samorì, P.; Ecker, C.; Gössl, I.; de Witte, P. A. J.; Cornelissen, J. J. L. M.; Metselaar, G. A.; Otten, M. B. J.; Rowan, A. E.; Nolte, R. J. M.; Rabe, J. P. *Macromolecules* **2002**, *35*, 5290−5294.

(4) (a) Zhang, H.; Grim, P. C. M.; Foubert, P.; Vosch, T.; Vanoppen, P.; Wiesler, U. M.; Berresheim, A. J.; Müllen, K.; De Schryver, F. C. *Langmuir* **2000**, *16*, 9009−9014. (b) Li, J.; Piehler, L. T.; Qin, D.; Baker, J. R.; Tomalia, D. A.; Meier, D. J. *Langmuir* **2000**, *16*, 5613−5616. (c) Drager, A. S.; Zangmeister, R. A. P.; Armstrong, N. R.; O'Brien, D. F. *J. Am. Chem. Soc.* **2001**, *123,* 3595−3596. (d) Kiriy, A.; Gorodyska, G.; Minko, S.; Jaeger, W.; Štěpánek, P.; Stamm, M. *J. Am. Chem. Soc.* **2002**, *124*, 13454−13462. (e) Kumaki, J.; Hashimoto, T. *J. Am. Chem. Soc.* **2003**, *125*, 4907−4917. (f) Li, B. S.; Cheuk, K. K. L.; Ling, L.; Chen, J.; Xiao, X.; Bai, C.; Tang, B. Z. *Macromolecules* **2003**, *36*, 77−85. (g) Sheiko, S. S.; da Silva, M.; Shirvaniants, D.; LaRue, I.; Prokhorova, S.; Möller, M.; Beers, K.; Matyjaszewski, K. *J. Am. Chem. Soc.* **2003**, *125*, 6725−6728.

(5) (a) Samorí, P.; Francke, V.; Müllen, K.; Rabe, J. P. *Chem.−Eur. J.* **1999**, *5*, 2312−2317. (b) Smolenyak, P.; Peterson, R.; Nebesny, K.; Törker, M.; O′Brien, D. F.; Armstrong, N. R. *J. Am. Chem. Soc.* **1999**, *121*, 8628−8636. (c) Schenning, A. P. H. J.; Kilbinger, A. F. M.; Biscarini, F.; Cavallini, M.; Cooper, H. J.; Derrick, P. J.; Feast, W. J.; Lazzaroni, R.; Leclere, Ph.; McDonell, L. A.; Meijer, E. W.; Meskers, S. C. J. *J. Am. Chem. Soc.* **2002**, *124*, 1269−1275. (d) Gössl, I.; Shu, L.; Schlüter, A. D.; Rabe, J. P. *J. Am. Chem. Soc.* **2002**, *124*, 6860−6865. (e) Luo, Y. H.; Liu, H. W.; Xi, F.; Li, L.; Jin, X. G.; Han, C. C.; Chan, C. M. *J. Am. Chem. Soc.* **2003**, *125*, 6447−6451.

(6) (a) Fritz, M.; Radmacher, M.; Cleveland, J. P.; Allerdma, M. W.; Stewart, R. J.; Gieselmann, R.; Janmey, P.; Schmidt, C. F.; Hansma, P. K. *Langmuir* **1995**, *11*, 3529−3535. (b) Schabert, F. A.; Rabe, J. P. *Biophys. J.* **1996**, *70*, 1514−1520. (c) Ji, X.; Oh, J.; Dunker, A. K.; Hipps, K. W. *Ultramicroscopy* **1998**, *72*, 165−176.

(7) Yang, G.; Vesenka, J. P.; Bustamante, C. J. *Scanning* **1996**, *18*, 344−350.

(8) (a) Kiriy, A.; Minko, S.; Gorodyska, G.; Stamm, M.; Jaeger, W. *Nano Lett.* **2002**, *2*, 881−885. (b) Minko, S.; Kiriy, A.; Gorodyska, A.; Stamm, M. *J. Am. Chem. Soc.* **2002**, *124*, 10192−10197. (c) Kiriy, A.; Gorodyska, G.; Minko, S.; Tsitsilianis, C.; Jaeger, W.; Stamm, M. *J. Am. Chem. Soc.* **2003**, *125*, 11202−11203.

(9) Van Noort, S. J. T.; Van der Werf, K. O.; De Grooth, B. G.; Van Hulst, N. F.; Greve, J. *Ultramicroscopy* **1997**, *69*, 117−127.

(10) Weisenhorn, A. L.; Maivald, P.; Butt, H.-J.; Hansma, P. K. *Phys. Rev. B.* **1992**, *45*, 11226−11232.

(11) Beaglehole, D.; Christenson, H. K. *J. Phys. Chem.* **1992**, *96*, 3359−3403.

(12) Thundat, T.; Zheng, X.-Y.; Chen, G. Y.; Warmack, R. J. *Surf. Sci. Lett.* **1993**, *294*, 939−943.

(13) (a) Bustamante, C.; Vesenka, J.; Tang, C. L.; Rees, W.; Guthold, M.; Keller, R. *Biochemistry* **1992**, *31*, 22−26. (b) Hansma, H. G.; Bezannilla, M, Zenhausern, F.; Adrian, M.; Sinsheimer, R. L. *Nucl. Acid Res.* **1993**, *21*, 505−512. (c) Rivetti, C.; Guthold, M.; Bustamante, C. *J. Mol. Biol.* **1996**, *264*, 919−932.

(14) (a) Thundat, T.; Warmack, R. J.; Alison, D. P.; Bottomley, L. A.; Lourenco, A. J.; Ferrell, T. L. *J. Vac. Sci. Technol. A* **1992**, *10*, 630−635. (b) Vesenka, J. P.; Manne, S.; Yang, G.; Bustamante, C. J.; Henderson, E. *Scan. Microsc.* **1993**, *7*, 781−788.

(15) Lyubchenko, Y. L.; Shlyakhtenko, L. S. *Proc. Natl. Acad. Sci. U.S.A.* **1997**, *94*, 496−501.

(16) Cornelissen, J. J. L. M.; Donners, J.; de Gelder, R.; Graswinckel, W. S.; Metselaar, G. A.; Rowan, A. E.; Sommerdijk, N. A. J. M.; Nolte, R. J. M. *Science* **2001**, *293*, 676−680.

(17) The water contact angle was found to be 70° at 25 °C, indicative of a slighly hydrophilic character of the polymer.

(18) Cornelissen, J. J. L. M.; Rowan, A. E.; Nolte, R. J. M.; Sommerdijk, N. A. J. M. *Chem. Rev.* **2001**, *101*, 4039−4070.

(19) Molecular Imaging Corportion, Tempe, AZ.

(20) Herminghaus, S.; Fery, A.; Reim, D. *Ultramicroscopy* **1997**, *69*, 211−217.

(21) Ecker, C. Ph.D. Thesis in preparation. Humboldt University Berlin.

(22) Shu, L.; Schlüter, A. D.; Ecker, C.; Severin, N.; Rabe, J. P. *Angew. Chem., Int. Ed.* **2001**, *40*, 4666−4669.
(23) Bustamante, C. J.; Erie, D. A.; Keller, D. *Curr. Opin. Struct. Biol.* **1994**, *4*, 750−760.
(24) Zitzler, L.; Herminghaus, S.; Mugele, F. *Phys. Rev. B* **2002**, *66*, 155436.
(25) (a) Müller, D. J.; Schabert, F. A.; Büldt, G.; Engel, A. *Biophys. J.* **1995**, *68*, 1681−1686. (b) Putman, C. A. J. *Development of an Atomic Force Microscope for Biological Applications*; University of Twente: Twente, The Netherlands, 1994.
(26) (a) Spatz, J. P.; Sheiko, S. S.; Möller, M. *Langmuir* **1997**, *13*, 4699−4703. (b) Spatz, J. P.; Sheiko, S. S.; Möller, M.; Winkler, R. G.; Reineker, P.; Marti, O. *Nanotechnology* **1995**, *6*, 40−44.
(27) Sarid, D. *Exploring Scanning Probe Microscopy with Mathematica.*; John Wiley & Sons Inc: New York, 1997.
(28) Zhuang, W.; Schlüter, A.-D.; Rabe, J. P. Unpublished results.

MA048786Z